# LS 44—An Improved Deep Space Network Station Location Set for Viking Navigation

H. M. Koble, G. E. Pease, K. W. Yip
Navigation Systems Section

*Improved estimates for the spin axis and longitude components of the Deep Space Network station locations have been obtained from post-flight processing of radio metric data received from various Mariner planetary missions. The use of an upgraded set of ionospheric calibrations and the incorporation of near-Venus and near-Mercury radio metric data from the Mariner 10 spacecraft are the principal contributing effects to the improvement. These new estimates, designated Location Set (LS) 44, have supported Viking navigation activities in the vicinity of Mars. As such, the station locations have been determined relative to the planetary positions inherent in JPL Development Ephemeris (DE) 84, which has been used throughout the Viking mission. The article also presents and discusses a version of LS 44 based upon the latest planetary ephemeris, DE 96.*

## I. Introduction

This article primarily focuses on an update which has recently been made to the location estimates for the Deep Space Network (DSN) tracking stations. The new solutions, designated Location Set (LS) 44, fulfill a requirement to provide the Viking mission with a "best" set of estimates to support critical navigation operations in the vicinity of Mars. As such, they replace LS 43 which had supported the launch and much of the interplanetary cruise phases of the mission.

The update was obtained by combining the absolute station location information inherent in radio metric data arcs received from five previous deep space probes (Mariners 4, 5, 6, 9, and 10) with relative position information from geodetic surveys at the various complexes. Adjustments were made only to the LS 43 estimates of each station's geocentric distance from the Earth's spin axis $r_s$ and geocentric longitude $\lambda$. The data under consideration, as expected, did not provide a sufficiently accurate absolute determination of the third coordinate, the geo-

centric height above Earth's equatorial plane Z, to warrant an update to the LS 43 values.[1]

Herein, emphasis will be placed on the differences between LS 43 and 44 with the intent of justifying why, in our view, the latter represents an improved spin axis and longitude determination. In brief, there are two principal reasons. First, the processing of radio metric data used to determine LS 43 has been improved, particularly in the area of calibrating the data to account for ionospheric charged particle effects. Second, new radio metric data have been incorporated into the combined data set solution thereby permitting the first accurate absolute determination of the locations for Deep Space Stations (DSS) 43 and 63. The new data, which are from the Mariner 10 mission, also enhance the estimates for other stations in the network.

Any set of DSN station location solutions is associated with some particular JPL planetary ephemeris. Both LS 43 and 44 are referenced to JPL Development Ephemeris (DE) 84. The second portion of the article will briefly discuss some results in connection with determining the effect of a planetary ephemeris update on the station location estimates, LS 44.

At present, if a new ephemeris is adopted during a mission, a *complete* reprocessing of the radio metric data must be performed in order to determine a set of station location estimates relative to the new ephemeris. A research project is currently in progress to develop an analytically based procedure that will enable us to adjust a set of station location estimates for ephemeris changes and circumvent the need for expensive data processing. Preliminary results have indicated that the Brouwer and Clemence Set III ephemeris partial derivatives can represent ephemeris differences to a level of accuracy commensurate with required station location accuracies. Therefore, a linear correction scheme using these partial derivatives appears promising. No matter what procedure is eventually developed, it will be necessary to test its accuracy against the complete reprocessing approach. Anticipating that this test will be made in the near future, the LS 44 data set was reprocessed using JPL Development Ephemeris 96, and a combined data solution was once again obtained for the spin axis and longitude components. The final portion of this article will compare the individual and combined solutions for DE 84 and DE 96.

[1]The coordinate system in question will be more fully described at the beginning of Section II.

## II. Background on Station Location Development Procedures

The locations of the DSN tracking stations are computed in a geocentric coordinate system whose axes are defined by the Earth mean pole (axis of rotation), equator, and prime meridian of 1903.0. A variety of coordinate parameters may be used to locate a given station within this system. At JPL, the cylindrical triplet $r_s$, $\lambda$, and Z is most often used,

where

$r_s$ = distance from the axis of rotation, km

$\lambda$ = longitude as measured east from the prime meridian, deg

Z = height above the equatorial plane, km

Figure 1 depicts the coordinate system and location parameters for one station.

Current station location development procedures are guided by a simplified, yet quite valuable theoretical analysis of the information content in the available radio metric data (primarily two-way doppler plus a relatively small number of range points). Details may be found in Refs. 1 and 2. The following discussion summarizes the general conclusions contained therein.

### A. Spin Axis Determination

In these references it is shown that uncertainties in the probe's absolute position (more precisely in the probe's declination) will degrade the spin axis estimate. Analysis reveals that if data are processed from either or both of two specific geometries, this correlation effect can be circumvented.

The first favorable geometry is one from which the probe's absolute position can be inferred independent of Earth-based parameters such as station locations. In theory, this can be done from data taken during the period of a probe's closest approach to a target body other than Earth—the so-called planetary encounter phase. During this period, a complete orbit estimate can be independently made because of the bending effect exerted on the probe's motion by the target planet's gravitational field. Processing the data only provides an accurate estimate of the probe's position *relative* to this planet. However, the necessary absolute reference is provided by the planetary ephemeris in usage.

Upon more careful study of the simplified, theoretical model used in this analysis, it can be noted that when the probe is at zero declination, an uncertainty in its position does not have an appreciable degrading effect on the information content of radio metric data for estimating $r_s$. Consequently, an absolute determination of the station's spin axis component can also be made if a short span of radio metric data is processed which includes a period when the probe's declination passes through zero degrees.

### B. Longitude Determination

In Ref. 2 it was demonstrated that station longitude accuracy depends heavily on the observability of the spacecraft's geocentric range rate, and the precision in the longitude estimate markedly improves as the range rate determination becomes more exact. Again, a planetary encounter geometry spanning a period of roughly encounter $\pm 5$ days should be useful for longitude work because the spacecraft absolute velocity can also be determined independent of Earth-based parameters. Unfortunately, in practice, the probe's encounter orbit velocity estimate may be degraded due to incomplete usable doppler tracking coverage, particularly from the post-encounter period. For example, if a large $\Delta V$ is required for orbit insertion (as in Mariner 9 and Viking), the post-insertion data cannot be combined with pre-insertion data to improve station location estimates. To reduce the velocity uncertainty and thereby improve the station longitude determination, a useful tactic is to supplement the usable doppler data with range measurements taken near the planetary encounter. This follows because range measured over time determines the mean range rate.

The Hamilton-Melbourne simplified, theoretical analysis (Ref. 1) indicates that the zero declination arc is not useful for determining accurate absolute longitude estimates. However, the relative difference in longitude between various stations will be preserved if solutions are obtained from this type of data arc.

### C. *Z* Height Determination

The Z component of station position is not well determined by doppler data. In order to produce a complete set of location estimates, it has been necessary to rely on data provided by sources outside JPL. Currently, we are using the results of geodetic surveys (Ref. 3) made at the various complexes and geocentric-geodetic differences prepared by Wolf Research Corporation (Ref. 4) using optical and laser data to obtain Z values. The Z height estimates were not changed from LS 43 to LS 44, and the values in current usage at JPL are displayed in Table 1. The use of existing Mariner range data and near-simultaneous range data from the Viking orbiters is currently being contemplated to improve the Z height determination.

### D. General Guidelines

Based on this theoretical analysis and past experience processing radio metric data, we can establish some general guidelines for determining the spin axis and longitude estimates.

(1) Define tracking arcs from the various missions that reflect the planetary encounter or zero declination geometry.

(2) For each arc, obtain the best set of calibrations for ionospheric charged particle effects, tropospheric refraction, and timing and polar motion which are currently available. Of course, our ability to obtain high-quality station spin axis and longitude estimates depends on minimizing the errors introduced by each of these sources.

(3) For each arc, obtain as accurate a spacecraft trajectory as possible.

(4) Given the best trajectory, obtain estimates for the spacecraft state at the initial epoch of each arc and estimates for the DSN stations which participated in tracking the given spacecraft during the defined time period. In this regard, it is usually necessary to simultaneously estimate one or more other parameter types such as solar pressure, planetary oblateness, range biases, attitude-control accelerations, planetary mass, etc.

(5) Combine the individual arc absolute station location determinations and any relative information from ground surveys to obtain a final set of estimates. Historically, the procedure used to perform this last step has varied, and we will defer any additional commentary until LS 43 and 44 are discussed.

## III. Location Set 43

The previous best set of station locations, Location Set 43, was announced in May 1975 and used to support the Viking mission during the launch and interplanetary cruise phase.

Table 2A and 2B summarizes the tracking arc geometry and radio metric data that provided the basis for the

spin axis and longitude estimates. As indicated, encounter arc data were used from the Mariner 4, 5, 6, and 9 missions along with a pre- and post-encounter zero declination phase of the Mariner 5 trajectory. The asymmetry relative to planetary encounter for Mariner 6 was due to unusable data caused by a gas-venting cooling operation; for Mariner 9 it was due to the Mars orbit insertion maneuver.

Each arc was processed using the orbit determination program of the Mariner 10 mission (Ref. 5); the same planetary ephemerides, JPL Development Ephemeris 84; the same source for UT1 (universal time) and Earth polar motion, the Bureau International de l'Heure (BIH); and the same model for tropospheric refraction calibrations.[2]

All doppler data were calibrated for the effects of ionospheric charged particles *with the exception* of the Mariner 4 data. Unfortunately, at the time of radio metric data processing for LS 43, calibrations were available only for a data set that was too small to provide reliable station location solutions. It was estimated that the errors introduced into the Mariner 4 solution by ignoring the ionospheric effect would be no more than $0.5 \times 10^{-5}$ deg (approximately ½ m) in longitude and 1.6 m in spin axis. The actual longitude error proved to be slightly larger than this prediction (see Table 8, right-most column).

Once the final individual arc solutions were obtained, LS 43 was produced by combining these six determinations in a least squares fashion. The final solution involved simultaneous estimation of 72 parameters: a six-dimensional spacecraft state vector for each arc (36 parameters); a three-dimensional solar pressure model vector for each arc (18 parameters); one range bias parameter for the Mariner 6 and 9 missions (2 parameters); and spin axis and longitude parameters for each of the eight stations, DSSs 11, 12, and 14 at Goldstone, 41 and 42 in Australia, 51 in South Africa, and 61 and 62 in Spain, which provided tracking coverage during the time periods in question (16 parameters).

In determining this final estimate, a priori information on station locations was included based on relative coordinate differences determined from ground-based geodetic surveys at the various complexes.[3] The geodetic data were transformed to the geocentric coordinate system defined in Fig. 1, and the results are presented in Table 3. The a priori spin axis and longitude absolute values conformed exactly with these differences, and the statistics on these values were defined by: standard deviation of the spin axis a priori values for survey-constrained stations, 1000 m, and for stations not constrained, 50 m; standard deviation of the longitude a priori values for survey-constrained stations, $1000 \times 10^{-5}$ deg, and for stations not constrained, $50 \times 10^{-5}$ deg; correlation coefficients determined to reflect a survey accuracy of 0.3 m and $0.3 \times 10^{-5}$ deg, respectively.

The final spin axis and longitude estimates are given in Table 4, and the differences between the individual data arc solutions and these values may be found in Table 5.

To provide a complete set of estimates for all stations in the Network, values for those which did not track (DSSs 13, 43, 44, and 63) were computed by adding the relative differences shown in the lower portion of Table 3 to the LS 43 solutions for the base stations at each site (DSSs 12, 42, and 61).

Using the data from Table 5, we conclude that for stations whose solution was based on more than one data arc, the consistency in spin axis estimates range from 1.090 m for DSS 51 to a worst case of 4.545 m for DSS 41. The Mariner 4 spin axis solutions are low because calibrations for ionospheric charged particle effects were not included.

The scatter for the encounter arc longitude estimates range from $1.200 \times 10^{-5}$ deg (~1.2 m) for DSS 41 to $4.296 \times 10^{-5}$ deg for DSS 51. The reader will note that the absolute longitude determinations from the zero-declination arcs are not consistent with the encounter arc solutions, particularly for the Mariner 5 postencounter case. These solutions, were included in the final LS 43

[2]JPL Development Ephemeris 84 was announced by E. M. Standish and M. S. W. Keesey of the Systems Division, Tracking System and Applications Section in an internal document, Interoffice Memorandum 391.5-553. The document is entitled, "Development Ephemeris 84 – Announcement," and was published on August 22, 1973.

A description of the data-gathering and data-processing system by which the timing and polar motion calibrations were obtained may be found in (Ref. 6).

Details concerning the mathematical model for tropospheric calibrations may be found in (Ref. 7). The "dry" and "wet" tropospheric zenith range error polynomials for each data arc were based on results discussed in a JPL document, Engineering Memorandum 391-506, prepared by F. B. Winn, C. C. Chao, and M. J. Richter.

[3]The survey data was obtained from (Ref. 3) and subsequent private communications between the DSN and N. A. Mottinger of the Systems Division, Navigation Systems Section.

determination; however, their formal uncertainties as computed by the orbit determination program are three to four times larger than the encounter arc statistics for comparable amounts of data. When LS 43 was prepared, the final estimates were interpreted to mean that these zero-declination longitude solutions would have minimal influence on the combined data estimates. Recent analysis has confirmed this hypothesis.

## IV. Location Set 44

Location Set 44 was announced in late April 1976 and has been used to support Viking mission activities since that time. This new set of station locations represents an update to the LS 43 spin axis and longitude estimates discussed in Section III. The differences between these solutions are primarily due to two factors: (1) the inclusion of radio metric data for two new encounter arcs and (2) an improved processing of the four encounter and two zero-declination arcs used to determine LS 43.

### A. New Radio Metric Data

Post-flight analysis of encounter arc data from the Mariner 10 mission had not been completed at the time the bulk of data processing for LS 43 was performed. A preliminary determination of station location estimates from the Venus and first Mercury encounters revealed that this new data would have a significant effect. By including it, the number of radio metric points on which a combined data arc solution would be based would more than double. Furthermore, since DSS 43 and 63 provided tracking coverage during these encounter arcs, the previous geodetic survey-based solutions could be augmented by absolute information from radio metric data.

The preliminary solutions for *both* encounter arcs indicated that a correction of approximately 3 m was warranted for the spin axis component of both DSS 42 and 43. This was due to the fact that the LS 43 value for DSS 42 was based on a paucity of ionospheric calibrated radio metric data from that station. As indicated in Table 2B, 358 points were incorporated; however, 276 of these from the Mariner 4 mission were uncalibrated. Since the LS 43 estimate for DSS 43 was obtained by adding a survey difference to the DSS 42 spin axis coordinates, we can say that the DSS 43 value was also based on primarily uncalibrated radio metric data.

A summary of the Mariner 10 data incorporated into the LS 44 solution is provided in Tables 6A and 6B. Range data were available for the Venus encounter arc, but analysis of a range + doppler based solution could not be completed in time to include in the LS 44 determination. Analysis subsequent to the generation of LS 44 revealed that if the doppler-only solution were replaced by this range + doppler solution, the effect on LS 44 would be to perturb the values by at most 0.09 m in spin axis and $0.31 \times 10^{-5}$ deg in longitude. An effort was also made to include data from the third encounter arc with Mercury. Unfortunately, examination of the residuals associated with filtering this data revealed that the quality of the fit was not very good and that further analysis and data processing would be needed before the Mercury 3 encounter could be included.

The doppler-only solution from the Venus encounter and the range + doppler solution from the first Mercury encounter will be discussed shortly.

### B. Improved Processing of LS 43 Data

The most significant factor which prompted a reprocessing of the radio metric data used to develop LS 43 was an upgrading of the set of calibrations for ionospheric charged particle effects. A complete discussion of these calibrations may be found in (Ref. 8). In summary, the following changes were made to the LS 43 data sets.

**1. Mariner 4 mission.** As noted in Section III, the radio metric data which were processed to obtain station location estimates from the Mariner 4 encounter arc were not calibrated for the ionospheric effect. For the LS 44 determination, calibrations were prepared directly from ionospheric total electron content (TEC) data wherever possible. Other radio metric data points were also calibrated by averaging available TEC data and mapping the resultant values to the appropriate time intervals and tracking stations-spacecraft lines of sight. Whereas 1015 uncalibrated doppler points were used in the LS 43 solution for the Mariner 4 mission, only 899 of these could be accurately calibrated for use in an LS 44 solution.

**2. Mariner 6 mission.** An analysis of the calibrations used for DSS 62 data revealed that the underlying TEC data were noisy and of poorer quality than data for other stations which tracked during the encounter arc period. It was decided to replace these calibrations with a new set prepared by averaging the available TEC data over the period from 7/26/69 to 7/30/69 and applying these averages to all of the radio metric data for DSS 62. These data were taken on 7/26 and 7/28. By using averaged

rather than actual TEC values, an additional 15 points could be calibrated.

**3. Mariner 9 mission.** At the time the Mariner 9 encounter arc data were processed for the LS 43 solution, calibrations were unavailable for one pass of data from DSS 41 taken on 11/11/71. A set of calibrations were prepared by averaging the total electron contents for the week including this date. In so doing, 39 additional points could be calibrated.

No modifications were made to the LS 43 ionospheric calibrations for any of the three Mariner 5 tracking arcs. In Table 7, we summarize the modifications which were made to the data sets used in preparing LS 43 (c.f. Table 2B).

Some minor modifications were made to the tropospheric calibrations, but the same planetary ephemeris DE 84 and timing and polar motion decks described previously for LS 43 were used in preparing LS 44.

### C. Procedure and Discussion of Individual Data Arc Solutions

Whereas the LS 43 solutions were obtained using the orbit determination program for the Mariner 10 mission, it was decided to use the corresponding program for the Viking mission to perform the data processing for LS 44. This was logical because LS 44 would be used to support the critical navigation activities for both Viking spacecraft in the vicinity of Mars.

As a first step, an effort was made to reproduce the individual data arc solutions of Table 5 (which were generated by the Mariner 10 orbit determination program) using the Viking software. That is to say, the upgraded calibrations for tropospheric and ionospheric effects were not initially used and internal constants from the Viking program were overridden by the corresponding Mariner values. In general, reproduceability was achieved to a very high accuracy (on the average, less than 0.2 meters in spin radius and $0.2 \times 10^{-5}$ degrees in longitude) with the notable exception of the Mariner 9 data arc. Extensive analysis (Ref. 8) revealed that the models for gas leaks did not correspond between the two programs, and that the Mariner 10 program did not handle the integration of its model in an entirely accurate manner. The discrepancy between the solutions from the two programs was as large as 0.26 meters in spin radius and $0.72 \times 10^{-5}$ deg in longitude.

In Table 8, we present a summary of the improved individual station location solutions which resulted from reprocessing the LS 43 data using the new software, upgraded calibrations for ionospheric and tropospheric effects, but same planetary ephemeris and timing and polar motion models. The left-hand columns contain the differences between these solutions and the LS 43 values of Table 4. The right-hand columns contain the differences between these solutions and the corresponding solutions from the original processing (i.e., the results of Table 5).

As anticipated, the average change in the solutions for the three Mariner 5 data arcs is much smaller than the adjustments to the Mariner 4-6-9 solutions. The sizeable increases in the spin radius and longitude estimates for Mariner 4, the dramatic change in the DSS 62 longitude estimate for Mariner 6, and the decreases in longitude estimates for Mariner 9 are, however, consistent with the ionospheric, tropospheric, and software gas leak model modifications discussed earlier.

The two Mariner 10 encounter arcs defined by Table 6A-B were also processed using the Viking software; the same ephemeris, JPL Development Ephemeris 84; BIH data for universal time and polar motion; and calibrations for ionosphere and troposphere generated by the same models which provided calibrations for the other data arcs. Table 9 summarizes the Mariner 10 solutions. The most significant effects are: (1) a large positive correction to the LS 43 spin axis estimates at DSS 42 and 43 and (2) a negative correction to the LS 43 longitude estimates of more than one meter. The apparent anomalies in the Mariner 10 Mercury 1 encounter solutions for $r_s$ at DSS 12 and $\lambda$ at DSS 42 are compensated by comparatively large uncertainties in these estimates (Table 9).

### D. Final Combined Solution

Once the final individual arc solutions were obtained, LS 44 was produced by combining these eight determinations in a direct, least squares fashion. The final solution involved estimation of: spin axis and longitude parameters for each of the ten stations, DSS 11, 12, 14, 41, 42, 43, 51, 61, 62, and 63 which provided tracking coverage during the time periods in question and the following set of parameters from the individual data arcs (these were the parameters which were simultaneously estimated with the participating stations in determining the individual arc estimates):

Mariner 4 encounter—a six-parameter spacecraft state

Mariner 5 preencounter—a six-parameter spacecraft state and a three-parameter solar pressure model vector

Mariner 5 encounter—same as Mariner 5 preencounter

Mariner 5 postencounter—same as Mariner 5 preencounter

Mariner 6 encounter—a six-parameter spacecraft state and one range bias parameter

Mariner 9 encounter—a six-parameter spacecraft state and one range bias parameter

Mariner 10 Venus encounter—a six-parameter spacecraft state, Venus oblateness, and mass of Venus

Mariner 10 Mercury 1 encounter—a six-parameter spacecraft state, Mercury oblateness, mass of Mercury, a nine-parameter solar pressure model vector, and four range bias parameters

In determining the final estimates, relative coordinate differences based on geodetic survey information were again included as a priori data. The a priori spin axis and longitude absolute values conformed exactly with the results of Table 3, and the statistics on these values were defined by: standard deviation of the spin axis a priori values, 50 m; standard deviation of the longitude a priori values, $50 \times 10^{-5}$ deg; correlation coefficients were determined to reflect an assumed survey accuracy of 0.3 m and $0.3 \times 10^{-5}$ deg, respectively.

The final spin axis and longitude estimates appear in Table 10. Since DSS 13 and 44 did not provide tracking coverage during the time periods in question, their estimates were computed by other means. For DSS 13, the geodetic survey-based relative spin axis and longitude differences (Table 3) were added to the LS 44 estimates for DSS 12. However, a different strategy was employed for DSS 44. This station provided tracking coverage for the Pioneer 10 spacecraft during its interplanetary cruise. Estimates for DSS 44 were obtained from this radio metric data, and it was found that they were not consistent with a spin axis and longitude determination based on the survey differences between DSS 42 and 44 as shown in Table 3. When solutions based on interplanetary cruise arc data from the Viking spacecrafts tended to confirm the Pioneer values, it was decided to abandon the survey information for DSS 44 minus DSS 42 in favor of this radio metric based solution. Consequently, the LS 44 values are the Pioneer absolute estimates.

Earlier we discussed the various factors which contribute to the differences between the LS 43 and 44 station location estimates. In Table 11, these differences are documented quantitatively. For each station in the network, we have computed the spin axis and longitude changes between the two location sets. These values appear in the left-most column of this table. In the center column, we show the effect of reprocessing the LS 43 data. A combined solution was obtained from the improved individual determinations documented in Table 8 using techniques identical to those for computing LS 44. The result was then differenced with the LS 43 solution. Finally, the right-most column of Table 11 shows the effect of adding Mariner 10 data to the combined solution resulting from the improved processing of LS 43 individual arcs. In other words, these values represent the difference between the left and center columns.

The most significant change between the LS 43 and 44 spin axis estimates occurs at DSS 42 and 43. Approximately 80% of this large positive increase is due to the Mariner 10 data. As noted earlier, this is not surprising; it had been predicted in preliminary post-flight analysis of this data. Most of the changes at the Goldstone complex (DSSs 11, 12, and 14) and South Africa (DSS 51) are due to reprocessing of LS 43 data. A glance at Table 8 reveals that the principal contributing factor was the addition of ionospheric calibrations for the Mariner 4 data arc.

The longitude changes from LS 43 to LS 44 are consistently negative. From the results of Table 9, it is clear that the Mariner 10 solutions would force the combined estimates in this direction. However, it is a little surprising to see that the reprocessing of LS 43 data also led to a negative shift in longitudes. Examining the Table 8 data, it would appear that the positive correction to the Mariner 4 estimates due to the ionospheric effect has been swamped by the large negative corrections in Mariner 9 resulting from proper handling of the gas leak model by Viking software and also by the very large change in the DSS 62 estimate for Mariner 6.

Recall that Table 8 and 9 also displayed the differences between the individual data arc solutions and the LS 43 estimates. We have represented the differences between these same solutions and the LS 44 estimates pictorially in Figs. 2 and 3. These differences are plotted against the number of Julian days past 1950.0. The time axis is an exact scale, and we have endeavored to center the results for each encounter arc about the encounter date. The Mariner 5 pre- (labeled M5C in the figures) and postencounter (labeled M5P in the figures) results have been placed in close proximity to the encounter arc

solutions for that mission. The horizontal line in the middle of each vertical bar represents the actual difference between the individual data arc solution for the indicated station and the LS 44 value. The size of the vertical bars reflect the formal 1-$\sigma$ (standard deviation) uncertainties for each individual solution which were produced by the Viking orbit determination program.

The longitude residuals appear to be drifting in a negative direction with time, although the slope seems to change following the Mariner 5 encounter. Although further analysis is needed, the spin axis residuals may be exhibiting a sinusoidal behavior.

## V. Effect of an Ephemeris Change on LS 44 Values

The set of station location estimates which we have designated as Location Set 44 were computed relative to the absolute planetary positions inherent in JPL Development Ephemeris 84. These estimates will not be valid if changes are made to the relative position of the Earth with the various encounter planets during the time periods specified by the data arcs used to obtain LS 44. A *rough* estimate of the changes in station locations due to an update of the adopted planetary ephemeris can be obtained from the differences in the respective geocentric right ascensions and declinations of the target planets at the times of spacecraft encounter. These numbers translate into equivalent changes in the DSS spin axis and longitude estimates according to

$$\Delta r_s = \frac{\Delta\delta}{206265} r_s \tan\delta$$

$$\Delta\lambda = \Delta\alpha$$

where $\Delta r_s$ is the change in spin axis for a given station due to the ephemeris change, $\Delta\lambda$ is the change in longitude for that station, $r_s$ is the spin axis estimate relative to the old ephemeris, $\delta$ is the target planet declination in degrees as defined by the old ephemeris, $\Delta\delta$ is the change in target planet declination between the old and new ephemeris in seconds of arc, and $\Delta\alpha$ is the change in target planet right ascension between the old and new ephemeris.

To illustrate this rough approximation scheme, let us assume the old ephemeris is DE 84, and the new ephemeris is JPL Development Ephemeris 96 (Ref. 9). The spin axis estimates $r_s$ relative to the old ephemeris will be the LS 44 values of Table 10. DE 84 based target planet declinations $\delta$ and the changes in planet declination $\Delta\delta$ and right ascension $\Delta\delta$ between the old and new ephemeris appear in Table 12A. These were computed at the various spacecraft encounter times. Using this data and the expressions for $\Delta r_s$ and $\Delta\lambda$ defined above, the approximate effect of this ephemeris change on the LS 44 spin axis and longitude values has been computed and appears in Table 12B.

However, a precise evaluation of the induced changes requires the "brute force" approach of reprocessing the individual arc tracking data to obtain station location estimates relative to the new ephemeris and combining the individual determinations to obtain a final location set. This has been done to the data which defines LS 44. For each arc, the inputs to the orbit determination program were not changed with the exception of replacing the DE 84 ephemeris and planetary partial derivative files with the corresponding ones for DE 96. Target planet centered initial conditions were used for the spacecraft state vector on each of the six encounter arc solutions. Heliocentric initial conditions were used for the Mariner 5 pre- and post-encounter solutions.

In Table 13, we show the actual differences between the individual data arc solutions for the DE 84 and DE 96 cases. Notice that for each data arc subsequent to and including the Mariner 5 post-encounter, the changes in spin axis and longitude induced by the ephemeris update are very nearly constant as the predictions of Table 12B suggest. However, there is no consistency to the changes in spin axis and longitude for each data arc preceding the Mariner 5 post-encounter. At present, we do not have a satisfactory explanation for this phenomenon.

The DE 96 based individual solutions have been combined using a procedure identical to the formation of LS 44. The resulting spin axis and longitude estimates appear in Table 14, and their differences with LS 44 are shown in Table 15.[4] The changes in spin axis are seen to be statistically insignificant. Consequently, from a station location viewpoint DE 96 induces a pure rotation of approximately $2.5 \times 10^{-5}$ deg East relative to DE 84 values.

[4]The DE 96 based station location solutions discussed herein have been computed using a value for the speed of light of 299792.5 km/sec. In the export version of DE 96 (Ref. 9) an updated value of 299792.458 km/s has been adopted. If the reader uses the updated value in all computations, we recommend that the Z values of Table 1 and the $r_s$ values of Table 14 be multiplied by the ratio 299792.458/299792.5 to obtain a DE 96 based station location set that is consistent with this new speed of light constant.

## VI. Summary

A preliminary determination of spin axis and longitude estimates based on radio metric data from the Viking 1 spacecraft indicates perturbations to the LS 44 values of, on the average, 1 m or less in $r_s$ and $1 \times 10^{-5}$ deg or less in $\lambda$. This tends to confirm our belief that the LS 44 spin axis and longitude values appearing in Table 10 represent an improved station location estimate. Previous deficiencies in calibrating the radio metric for ionospheric charged particle effects have been minimized and new, useful data from the Mariner 10 mission have been incorporated. As summarized by Table 11, the net effect has been to increase previous spin axis estimates, particularly for DSSs 42 and 43, and to shift the longitude estimates westward.

Our study also reveals that if the latest planetary ephemeris, JPL Development Ephemeris 96 is adopted, the effect on station location estimates, as summarized in Table 15, will be to rotate the system approximately $2.5 \times 10^{-5}$ degrees eastward.


## Acknowledgement

The authors wish to acknowledge N. A. Mottinger for his contributions to the determination of LS 43, the reduction of geodetic survey information, and the development of combination software for LS 44. G. C. Rinker served as the primary consultant for Viking software used in the individual data arc processing. K. H. Rourke designed and coordinated the activities for developing the improved station locations described in this article.

# References


1. Hamilton, T. W., and Melbourne, W. G., "Information Content of a Single Pass of Doppler Data from a Distant Spacecraft," in *The Deep Space Network*, Space Program Summary 37-39, Vol. III, pp. 18–23. Jet Propulsion Laboratory, Pasadena, Calif., May 31, 1966.

2. Rourke, K. H., and Mottinger, N. A., "Resolution of an Inconsistency in Deep Space Station Longitude Solutions," in *The Deep Space Network Progress Report 42-44*, pp. 132–143. Jet Propulsion Laboratory, Pasadena, Calif., December 15, 1974.

3. NASA Directory of Observation Station Locations, Vol. 1, 3rd Ed., Goddard Space Flight Center, November 1973.

4. Marsh, J. G., Douglas, B. C., and Losko, S. M., *A Global Station Coordinate Solution Based upon Camera and Laser Data—Goddard Space Flight Center 1973*, Report X-592-72-177, p. 61, May 1973.

5. MVM'73 MOS Software Orbit Determination Program (ODP) Requirements, SRD-73-3-482, July 11, 1972 (JPL internal document).

6. Fliegel, H. F. and Wimberly, R. N., *Tracking System Analytic Calibration Activities for the Mariner Mars 1971 Mission*, Technical Report 32-1587, pp. 77–82. Jet Propulsion Laboratory, Pasadena, Calif., March 1, 1974.

7. Chao, C. C., *Tracking System Analytic Calibration Activities for the Mariner Mars 1971 Mission*, Technical Report 32-1587, pp. 61–77, Jet Propulsion Laboratory, March 1, 1974.

8. Yip, K. W., "LS 43 Updates for LS 44," to appear in *The Deep Space Network Progress Report.*

9. Standish, E. M., Keesey, M. S. W., and Newhall, X. X., *JPL Development Ephemeris Number 96*, Technical Report 32-1603, Jet Propulsion Laboratory, Pasadena, Calif., Feb. 19, 1976.

**Table 1. Current Z heights estimates LS 43 and LS 44**

| DSS | Z, km |
|---|---|
| 11 | 3673.765 |
| 12 | 3665.629 |
| 13 | 3660.957 |
| 14 | 3667.053 |
| 41 | −3302.189 |
| 42 | −3674.589 |
| 43 | −3674.756 |
| 44 | −3691.410 |
| 51 | −2768.744 |
| 61 | 4114.879 |
| 62 | 4116.902 |
| 63 | 4115.105 |

**Table 2A. Summary of tracking arc geometry, LS 43**

| Mission | Tracking arc | Encounter date | Target planet | a | b | c |
|---|---|---|---|---|---|---|
| Mariner 4 encounter | 1965 7/6–7/28 | 1965 7/15 | Mars | 12 h 31 min | 1.45 | −3 |
| Mariner 5 preencounter | 1967 7/22–9/16 | – | – | – | – | −8 to 8 |
| Mariner 5 encounter | 1967 10/14–10/25 | 1967 10/19 | Venus | 10 h 46 min | 0.53 | 6 |
| Mariner 5 postencounter | 1967 10/29–11/21 | – | – | – | – | 2 to −2 |
| Mariner 6 encounter | 1969 7/25–7/31 | 1969 7/31 | Mars | 16 h 10 min | 0.64 | −24 |
| Mariner 9 encounter | 1971 11/9–11/13 | 1971 11/14 | Mars | 22 h 27 min | 0.81 | −12 |

[a]Apparent right ascension of target plane at encounter date, JPL Development Ephemeris 84

[b]True distance from Earth to target planet at encounter date (AU), JPL Development Ephemeris 84

[c]Spacecraft declination (deg)

**Table 2B. Number of data points for each station, LS 43**

| Mission | Participating DSS | Number of data points by type | |
|---|---|---|---|
| Mariner 4 encounter | 11 | 501 F2 | |
| | 42 | 276 F2 | |
| | 51 | 238 F2 | |
| Mariner 5 preencounter | 11 | 104 F2 | |
| | 12 | 44 F2 | |
| | 14 | 101 F2 | |
| | 42 | 82 F2 | |
| | 61 | 504 F2 | |
| | 62 | 151 F2 | |
| Mariner 5 encounter | 12 | 148 F2 | |
| | 14 | 388 F2 | |
| | 41 | 48 F2 | |
| | 62 | 175 F2 | |
| Mariner 5 postencounter | 12 | 242 F2 | |
| | 14 | 121 F2 | |
| | 41 | 99 F2 | |
| | 62 | 242 F2 | |
| Mariner 6 encounter | 12 | 283 F2 | |
| | 14 | 53 F2 | 332 Tau |
| | 41 | 201 F2 | |
| | 51 | 26 F2 | |
| | 62 | 64 F2 | |
| Mariner 9 encounter | 12 | 152 F2 | 6 Mu |
| | 14 | 29 F2 | |
| | 41 | 155 F2 | |
| | 62 | 423 F2 | |

F2 = two-way doppler, S-band
Tau = Tau range data
Mu = Mu range data

**Table 3. Relative coordinate differences based on geodetic survey information**

| Station pair | $\Delta r_s$, km | $\Delta\lambda$, deg |
|---|---|---|
| 11–12 | −5.71166 | −0.0439311 |
| 14–12 | −8.05467 | −0.0840455 |
| 62–61 | −1.79030 | −0.1188072 |
| 13–12 | 3.43285 | 0.0105998 |
| 43–42 | −0.10110 | 0.0 |
| 44–42 | −11.37185 | −0.0034758 |
| 63–61 | −0.15712 | −0.0010142 |

**Table 4. Spin axis and longitude values, LS 43**

| DSS | $r_s$, km | $\lambda$, deg East |
|---|---|---|
| 11 | 5206.340339 | 243.1505977 |
| 12 | 5212.052093 | 243.1945268 |
| 14 | 5203.997323 | 243.1104843 |
| 41 | 5450.203649 | 136.8874971 |
| 42 | 5205.349548 | 148.9812787 |
| 51 | 5742.939590 | 27.6854314 |
| 61 | 4862.608422 | 355.7509853 |
| 62 | 4860.818264 | 355.6321788 |
| 13 | 5215.484943 | 243.2051266 |
| 43 | 5205.248448 | 148.9812787 |
| 44 | 5193.977698 | 148.9778029 |
| 63 | 4862.451302 | 355.7519995 |

**Table 5. Individual data arc solutions minus LS 43 values**

| DSS | Mission | $\Delta r_s$, m | $\Delta\lambda$, $10^{-5}$ deg |
|---|---|---|---|
| 11 | Mariner 4 encounter | −0.972 | 2.044 |
| | Mariner 5 preencounter | 1.403 | 1.856 |
| 12 | Mariner 5 preencounter | 1.750 | 1.939 |
| | Mariner 5 encounter | 0.672 | −1.322 |
| | Mariner 5 postencounter | 0.274 | 9.192 |
| | Mariner 6 encounter | −2.562 | 0.262 |
| | Mariner 9 encounter | −1.035 | −1.090 |
| 14 | Mariner 5 preencounter | 0.470 | 2.807 |
| | Mariner 5 encounter | −0.127 | −1.833 |
| | Mariner 5 postencounter | −1.361 | 9.699 |
| | Mariner 6 encounter | −1.362 | 0.257 |
| | Mariner 9 encounter | 1.997 | −1.703 |
| 41 | Mariner 5 encounter | −2.373 | −0.332 |
| | Mariner 5 postencounter | −1.985 | 10.692 |
| | Mariner 6 encounter | −1.880 | −0.195 |
| | Mariner 9 encounter | 2.172 | −1.395 |
| 42 | Mariner 4 encounter | 0.042 | 1.295 |
| | Mariner 5 preencounter | 1.733 | 2.368 |
| 51 | Mariner 4 encounter | 0.174 | 1.641 |
| | Mariner 6 encounter | 1.264 | −2.655 |
| 61 | Mariner 5 preencounter | 0.060 | 2.127 |
| 62 | Mariner 5 preencounter | 0.091 | 0.441 |
| | Mariner 5 encounter | −0.482 | −1.563 |
| | Mariner 5 postencounter | −0.840 | 9.918 |
| | Mariner 6 encounter | 0.066 | 2.215 |
| | Mariner 9 encounter | 1.818 | −1.507 |

**Table 6A. Summary of tracking arc geometry from the Mariner 10 mission used in LS 44**

| Mission | Tracking date | Encounter date | Target planet | a | b | c |
|---|---|---|---|---|---|---|
| Mariner 10 Venus encounter | 1974 1/28–2/14 | 1974 2/5 | Venus | 19 h 51 min | 0.29 | −13 |
| Mariner 10 1st Mercury encounter | 1974 3/21–4/10 | 1974 3/29 | Mercury | 22 h 52 min | 0.98 | −9 |

[a]Apparent right ascension of target planet at encounter date, JPL Development Ephemeris 84

[b]True distance from Earth to target planet at encounter date (AU), JPL Development Ephemeris 84

[c]Spacecraft declination (deg)

**Table 6B. Number of data points for each station Mariner 10 encounter arcs**

| Mission | Participating DSS | Number of data points by type | |
|---|---|---|---|
| Mariner 10 Venus encounter | 12 | 384 F2 | |
| | 14 | 934 F2 | |
| | 42 | 121 F2 | |
| | 43 | 1415 F2 | |
| | 62 | 347 F2 | |
| | 63 | 961 F2 | |
| Mariner 10 1st Mercury encounter | 12 | 181 F2 | 3 Plop |
| | 14 | 425 F2 | 43 Mu2 |
| | 42 | 62 F2 | |
| | 43 | 575 F2 | 30 Plop |
| | 62 | 64 F2 | |
| | 63 | 564 F2 | 35 Plop |

F2 = two-way doppler, S band
Mu2 = Mu2 range data
Plop = planetary operational ranging points

**Table 7. Modifications to the number of data points for each station, LS 43 vs. LS 44**

| Mission | Participating DSS | Number of data points by type | | | |
|---|---|---|---|---|---|
| | | LS 43 | | LS 44 | |
| Mariner 4 encounter | 11 | 501 F2 | | 473 F2 | |
| | 42 | 276 F2 | | 245 F2 | |
| | 51 | 238 F2 | | 181 F2 | |
| Mariner 6 encounter | 12 | 238 F2 | | 283 F2 | |
| | 14 | 53 F2 | 332 Tau | 53 F2 | 322 Tau |
| | 41 | 201 F2 | | 201 F2 | |
| | 51 | 26 F2 | | 26 F2 | |
| | 62 | 64 F2 | | 79 F2 | |
| Mariner 9 encounter | 12 | 152 F2 | 6 Mu | 152 F2 | 6 Mu |
| | 14 | 29 F2 | | 29 F2 | |
| | 41 | 155 F2 | | 194 F2 | |
| | 62 | 423 F2 | | 423 F2 | |

**Table 8. Changes due to improved processing of LS data**

| Mission | Participating DSS | Comparison of improved solutions with LS 43 values[a] | | Comparison of improved solutions with individual solutions used in LS 43[b] | |
|---|---|---|---|---|---|
| | | $\Delta r_s$, m | $\Delta\lambda$, $10^{-5}$ deg | $\Delta r_s$, m | $\Delta\lambda$, $10^{-5}$ deg |
| Mariner 4 encounter | 11 | 0.522 | 2.940 | 1.494 | 0.896 |
| | 42 | 0.485 | 2.107 | 0.443 | 0.812 |
| | 51 | 0.846 | 2.376 | 0.672 | 0.735 |
| Mariner 5 preencounter | 11 | 1.549 | 1.952 | 0.146 | 0.096 |
| | 12 | 1.966 | 1.850 | 0.216 | 0.089 |
| | 14 | 0.666 | 2.939 | 0.196 | 0.132 |
| | 42 | 1.844 | 2.515 | 0.111 | 0.147 |
| | 61 | 0.292 | 2.226 | 0.232 | 0.099 |
| | 62 | 0.377 | 0.799 | 0.286 | 0.358 |
| Mariner 5 encounter | 12 | 0.700 | −1.488 | 0.028 | −0.166 |
| | 14 | −0.062 | −1.715 | 0.065 | 0.118 |
| | 41 | −2.196 | −0.363 | 0.177 | −0.031 |
| | 62 | −0.393 | −1.708 | 0.089 | −0.145 |
| Mariner 5 postencounter | 12 | 0.227 | 9.396 | −0.047 | 0.204 |
| | 14 | −1.427 | 9.948 | −0.066 | 0.249 |
| | 41 | −1.976 | 10.664 | 0.009 | −0.028 |
| | 62 | −0.749 | 10.100 | 0.091 | 0.182 |
| Mariner 6 encounter | 12 | −2.199 | −0.183 | 0.363 | −0.445 |
| | 14 | −1.203 | −0.078 | 0.159 | −0.335 |
| | 41 | −1.811 | −0.580 | 0.069 | −0.385 |
| | 51 | 1.192 | −2.895 | −0.072 | −0.240 |
| | 62 | −0.234 | 0.270 | −0.300 | −1.945 |
| Mariner 9 encounter | 12 | −1.093 | −1.760 | −0.058 | −0.670 |
| | 14 | 1.731 | −2.431 | −0.266 | −0.728 |
| | 41 | 2.120 | −1.731 | −0.052 | −0.336 |
| | 62 | 1.707 | −2.303 | −0.111 | −0.796 |

[a] $\Delta r_s = r_s$ (improved) − $r_s$ (LS 43)
$\Delta\lambda = \lambda$ (improved) − $\lambda$ (LS 43)

[b] $\Delta r_s = r_s$ (improved) − $r_s$ (original)
$\Delta\lambda = \lambda$ (improved) − $\lambda$ (original)

**Table 9. Mariner 10 station location solutions used in LS 44**

| Mission | Participating DSS | $\Delta r_s$, m[a] | Std Dev, m[c] | $\Delta\lambda$, $10^{-5}$ deg[b] | Std Dev, $10^{-5}$ deg[c] |
|---|---|---|---|---|---|
| Mariner 10 Venus encounter | 12 | 0.571 | 0.618 | −1.723 | 0.755 |
| | 14 | 0.249 | 0.550 | −2.296 | 0.697 |
| | 42 | 2.815 | 1.243 | −1.673 | 1.090 |
| | 43 | 3.212 | 0.305 | −1.460 | 0.660 |
| | 62 | 0.968 | 0.651 | −2.539 | 0.837 |
| | 63 | 0.961 | 0.403 | −1.486 | 0.712 |
| Mariner 10 1st Mercury encounter | 12 | 2.685 | 2.093 | −2.776 | 1.240 |
| | 14 | 0.628 | 0.486 | −1.981 | 0.308 |
| | 42 | 4.808 | 1.555 | 4.808 | 1.413 |
| | 43 | 3.443 | 0.322 | −0.279 | 0.275 |
| | 62 | 1.132 | 1.035 | −0.677 | 0.817 |
| | 63 | 0.282 | 0.352 | −2.230 | 0.292 |

[a]$\Delta r_s = r_s$ (individual solution) $- r_s$ (LS 43)

[b]$\Delta\lambda = \lambda$ (individual solution) $- \lambda$ (LS 43)

[c]These are the formal standard deviations (1-$\sigma$) of the non-consider parameter estimates of the station locations as produced by the Viking orbit determination program.

**Table 10. Spin axis and longitude values, LS 44**

| DSS | $r_s$, km | $\lambda$, deg East |
|---|---|---|
| 11 | 5206.340852 | 243.1505848 |
| 12 | 5212.052472 | 243.1945123 |
| 14 | 5203.997735 | 243.1104678 |
| 41 | 5450.203703 | 136.8874855 |
| 42 | 5205.352165 | 148.9812708 |
| 43 | 5205.251697 | 148.9812726 |
| 51 | 5742.940160 | 27.6854256 |
| 61 | 4862.608849 | 355.7509710 |
| 62 | 4860.818670 | 355.6321631 |
| 63 | 4862.451845 | 355.7519840 |
| 13 | 5215.485322 | 243.2051121 |
| 44 | 5193.986790 | 148.9778162 |

**Table 11. Analysis of the spin axis and longitude update**

| | Participating DSS | LS 44–LS 43 | Effect of improved processing of LS 43 data | Effect of Mariner 10 data |
|---|---|---|---|---|
| Spin axis, m | 11 | 0.51 | 0.44 | 0.07 |
| | 12 | 0.38 | 0.28 | 0.10 |
| | 14 | 0.41 | 0.28 | 0.13 |
| | 41 | 0.05 | 0.12 | −0.07 |
| | 42 | 2.62 | 0.56 | 2.06 |
| | 43 | 3.15 | 0.46 | 2.69 |
| | 51 | 0.57 | 0.63 | −0.06 |
| | 61 | 0.43 | 0.23 | 0.20 |
| | 62 | 0.41 | 0.14 | 0.28 |
| | 63 | 0.56 | 0.28 | 0.28 |
| Longitude, $10^{-5}$ deg | 11 | −1.29 | −0.64 | −0.65 |
| | 12 | −1.45 | −0.70 | −0.75 |
| | 14 | −1.65 | −0.65 | −1.00 |
| | 41 | −1.16 | −0.47 | −0.69 |
| | 42 | −0.79 | −0.58 | −0.21 |
| | 43 | −0.61 | −0.58 | −0.03 |
| | 51 | −0.59 | −0.46 | −0.13 |
| | 61 | −1.43 | −0.75 | −0.68 |
| | 62 | −1.57 | −0.80 | −0.77 |
| | 63 | −1.58 | −0.77 | −0.81 |

**Table 12A. Target planet ephemeris parameters**

| Mission | Target planet declination, DE 84, deg | $\Delta\delta$, arc-sec | $\Delta\alpha$, arc-sec |
|---|---|---|---|
| Mariner 4 encounter | −3.1897 | −0.0265612 | 0.0684338 |
| Mariner 5 encounter | 6.2464 | −0.0301313 | 0.0727104 |
| Mariner 6 encounter | −24.4210 | −0.0530386 | 0.0708131 |
| Mariner 9 encounter | −11.505 | −0.0267841 | 0.1103786 |
| Mariner 10 Venus encounter | −13.2284 | −0.0492917 | 0.109137 |
| Mariner 10 1st Mercury encounter | −9.3958 | 0.0308986 | 0.0905302 |

Target planet declinations are relative to spacecraft encounter times.

$\alpha$ = target planet right ascension, $\delta$ = target planet declination.

$\Delta\alpha = \alpha(\text{DE } 96) - \alpha(\text{DE } 84)$, at spacecraft encounter time.

$\Delta\delta = \delta(\text{DE } 96) - \delta(\text{DE } 84)$, at spacecraft encounter time.

**Table 12B. Predicted effect of an ephemeris update on station Location Set 44 (DE 96 minus DE 84 individual data arc solutions)**

| | Participating DSS | Mariner 4 encounter | Mariner 5 encounter | Mariner 6 encounter | Mariner 9 encounter | Mariner 10 encounter | Mariner 10 Mercury 1 encounter |
|---|---|---|---|---|---|---|---|
| Spin axis, m | 11 | 0.04 | | | | | |
| | 12 | | −0.08 | 0.61 | 0.14 | 0.29 | −0.13 |
| | 14 | | −0.08 | 0.61 | 0.14 | 0.29 | −0.13 |
| | 41 | | −0.09 | 0.64 | 0.14 | | |
| | 42 | 0.04 | | | | 0.29 | −0.13 |
| | 43 | | | | | 0.29 | −0.13 |
| | 51 | 0.04 | | 0.67 | | | |
| | 61 | | | | | | |
| | 62 | | −0.08 | 0.57 | 0.13 | 0.27 | −0.12 |
| | 63 | | | | | 0.27 | −0.12 |
| Longitude, $10^{-5}$ deg | 11 | 1.90 | | | | | |
| | 12 | | 2.02 | 1.97 | 3.07 | 3.03 | 2.51 |
| | 14 | | 2.02 | 1.97 | 3.07 | 3.03 | 2.51 |
| | 41 | | 2.02 | 1.97 | 3.07 | | |
| | 42 | 1.90 | | | | 3.03 | 2.51 |
| | 43 | | | | | 3.03 | 2.51 |
| | 51 | 1.90 | | 1.97 | | | |
| | 61 | | | | | | |
| | 62 | | 2.02 | 1.97 | 3.07 | 3.03 | 2.51 |
| | 63 | | | | | 3.03 | 2.51 |

**Table 13. True effect of an ephemeris update on station Location Set 44 (DE 96 minus DE 84 individual data arc solutions)**

| | Participating DSS | Mariner 4 encounter | Mariner 5 pre-encounter | Mariner 5 encounter | Mariner 5 post-encounter | Mariner 6 encounter | Mariner 9 encounter | Mariner 10 Venus encounter | Mariner 10 Mercury 1 encounter |
|---|---|---|---|---|---|---|---|---|---|
| Spin axis, m | 11 | −0.585 | 0.200 | | | | | | |
| | 12 | | 0.151 | −0.410 | 0.000 | 0.284 | 0.278 | 0.279 | −0.164 |
| | 14 | | −0.005 | −0.250 | 0.004 | 0.326 | 0.234 | 0.261 | −0.119 |
| | 41 | | | 0.598 | −0.040 | 0.395 | 0.254 | | |
| | 42 | 0.330 | 0.054 | | | | | 0.284 | −0.168 |
| | 43 | | | | | | | 0.272 | −0.122 |
| | 51 | −0.094 | | | | 0.398 | | | |
| | 61 | | 0.018 | | | | | | |
| | 62 | | 0.176 | −0.052 | 0.004 | 0.407 | 0.216 | 0.260 | −0.141 |
| | 63 | | | | | | | 0.267 | −0.101 |
| Longitude, $10^{-5}$ deg | 11 | 3.502 | 1.937 | | | | | | |
| | 12 | | 2.661 | 1.648 | 2.345 | 2.141 | 3.412 | 3.142 | 2.537 |
| | 14 | | 1.943 | 1.495 | 2.339 | 2.166 | 3.390 | 3.121 | 2.496 |
| | 41 | | | 1.826 | 2.292 | 2.146 | 3.350 | | |
| | 42 | 2.354 | 1.615 | | | | | 3.152 | 2.434 |
| | 43 | | | | | | | 3.107 | 2.503 |
| | 51 | 2.634 | | | | 2.213 | | | |
| | 61 | | 1.921 | | | | | | |
| | 62 | | 3.333 | 1.728 | 2.338 | 2.187 | 3.404 | 3.186 | 2.498 |
| | 63 | | | | | | | 3.111 | 2.493 |

**Table 14. Spin axis and longitude values — combined solution for DE 96**

| DSS | $r_s$, km | λ, deg East |
|---|---|---|
| 11 | 5206.340775 | 243.1506103 |
| 12 | 5212.052461 | 243.1945377 |
| 14 | 5203.997723 | 243.1104930 |
| 41 | 5450.203863 | 136.8875110 |
| 42 | 5205.352285 | 148.9812947 |
| 43 | 5205.251765 | 148.9812975 |
| 51 | 5742.940200 | 27.6854493 |
| 61 | 4862.608909 | 355.7509964 |
| 62 | 4860.818730 | 355.6321890 |
| 63 | 4862.451921 | 355.7520093 |
| 13 | 5215.485311 | 243.2051375 |

**Table 15. Effect of an ephemeris update on station locations (combined DE 96 solution minus LS 44 values)**

| DSS | $\Delta r_s$, m | $\Delta\lambda$, $10^{-5}$ deg |
|---|---|---|
| 11 | −0.077 | 2.55 |
| 12 | −0.011 | 2.54 |
| 14 | −0.012 | 2.52 |
| 41 | 0.160 | 2.55 |
| 42 | 0.120 | 2.39 |
| 43 | 0.068 | 2.49 |
| 51 | 0.040 | 2.37 |
| 61 | 0.060 | 2.54 |
| 62 | 0.060 | 2.59 |
| 63 | 0.076 | 2.53 |

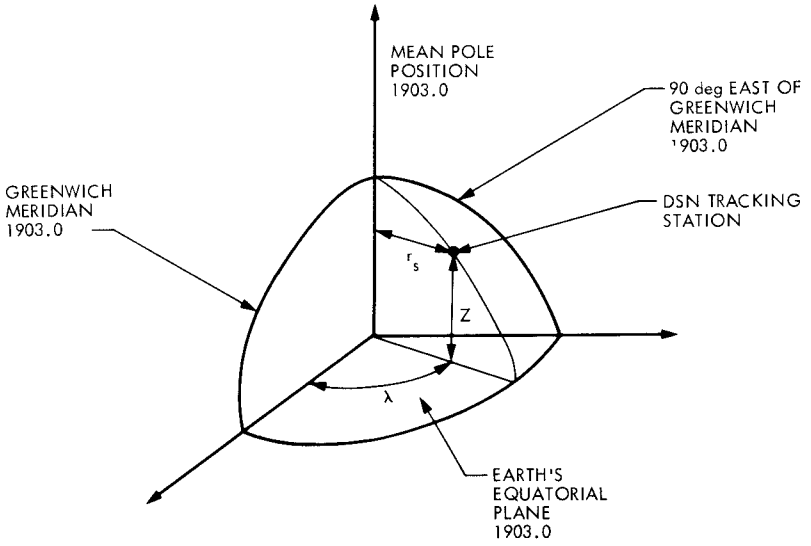


Fig. 1. A cylindrical coordinate system for locating a DSN station

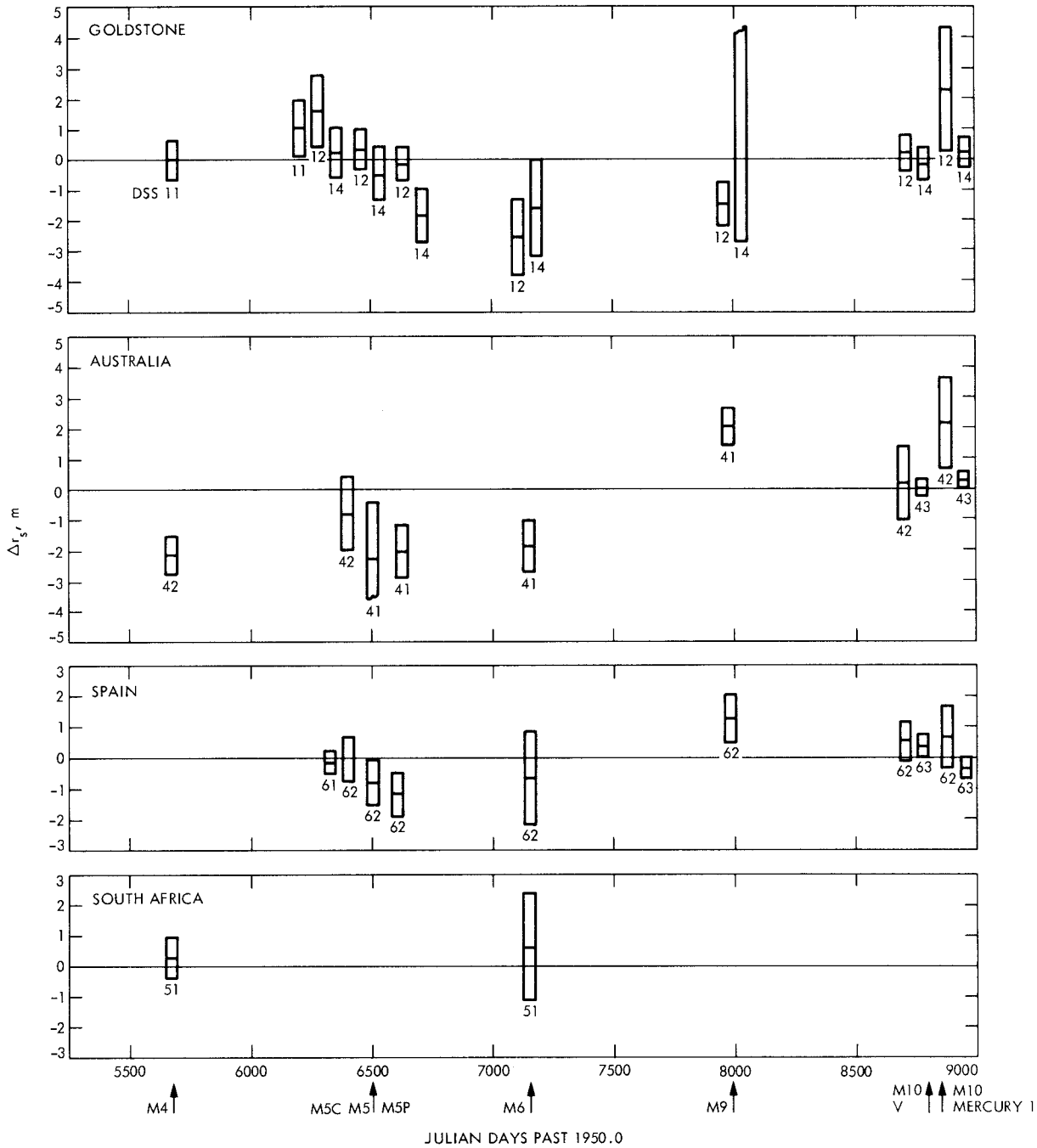


**Fig. 2. Differences between individual data arc spin axis estimates and LS 44 values**

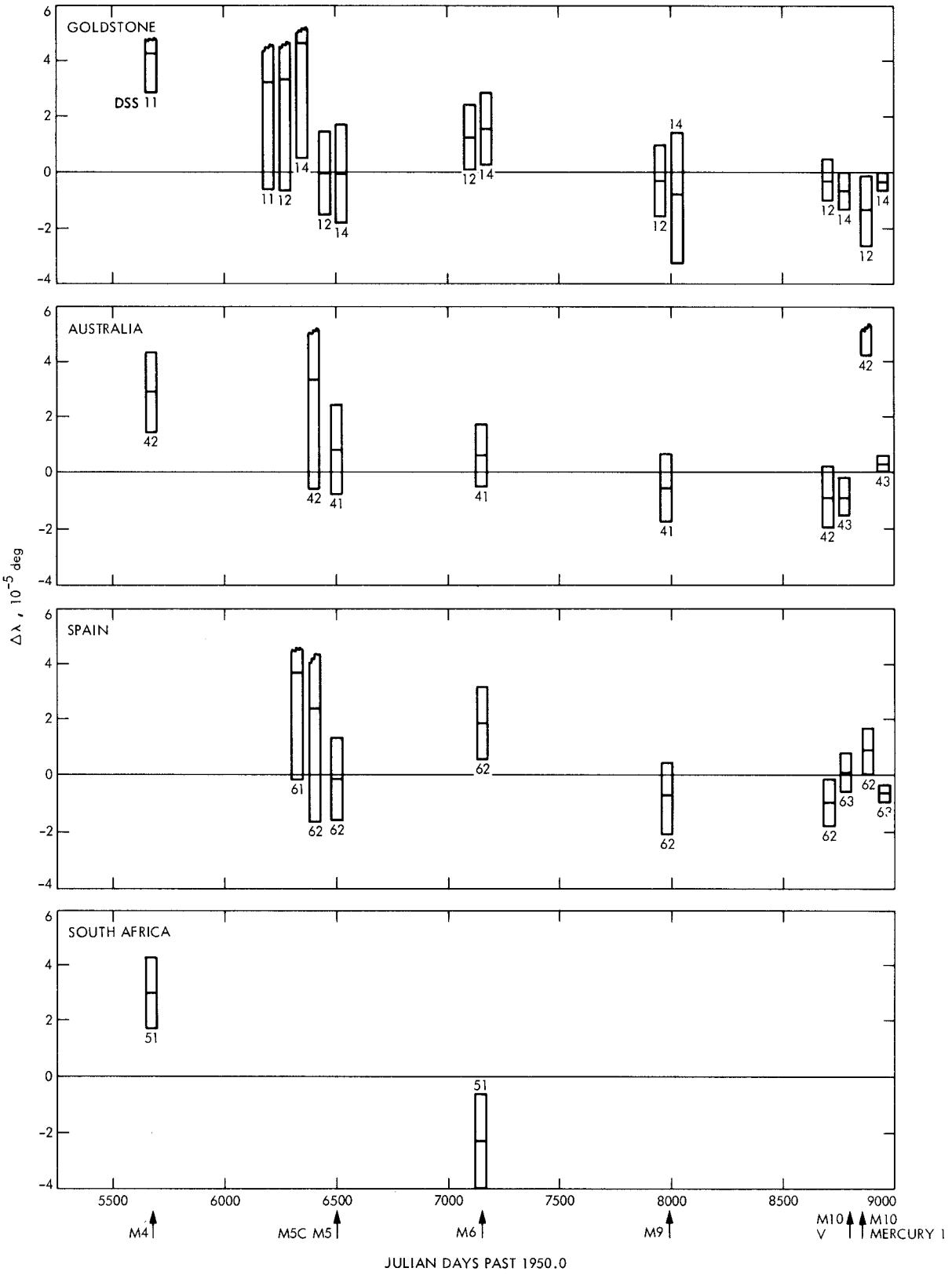


Fig. 3. Differences between individual data arc longitude estimates and LS 44 values